Pressure induced magnetic and semiconductor–metal phase transitions in Cr_2MoO_6*

San-Dong Guo(郭三栋)†

Department of Physics, School of Sciences, China University of Mining and Technology, Xuzhou 221116, *China*

(Received 14 December 2015; revised manuscript received 8 January 2016; published online 1 April 2016)

We investigate magnetic ordering and electronic structures of Cr_2MoO_6 under hydrostatic pressure. To overcome the band gap problem, the modified Becke and Johnson exchange potential is used to investigate the electronic structures of Cr_2MoO_6. The insulating nature at the experimental crystal structure is produced, with a band gap of 1.04 eV, and the magnetic moment of the Cr atom is 2.50 μ_B, compared to an experimental value of about 2.47 μ_B. The calculated results show that an antiferromagnetic inter-bilayer coupling–ferromagnetic intra-bilayer coupling to a ferromagnetic inter-bilayer coupling–antiferromagnetic intra-bilayer coupling phase transition is produced with the pressure increasing. The magnetic phase transition is simultaneously accompanied by a semiconductor–metal phase transition. The magnetic phase transition can be explained by the Mo–O hybridization strength, and ferromagnetic coupling between two Cr atoms can be understood by empty Mo-d bands perturbing the nearest O-p orbital.

Keywords: magnetic phase transition, pressure, magnetic coupling mechanism

PACS: 71.30.+h, 71.20.−b, 75.50.−y, 75.90.+w **DOI:** 10.1088/1674-1056/25/5/057104

1. Introduction

Many interesting phenomena can be produced by using the pressure, such as semiconductor to metal,[1] conventional insulator to topological insulator,[2–4] and ferromagnetic semiconductor to spin gapless semiconductor[5] transitions. Exploring the magnetic coupling mechanism in magnetic materials has always been a fundamental topic.[6–10] The exchange coupling in transition-metal oxides can be understood by the superexchange interaction,[6] and the double-exchange mechanism[7] which can explain the metallicity and ferromagnetic coupling in the mixed-valence Mn compounds.

The inverse-trirutile compounds Cr_2XO_6 (X = W, Te, Mo) with space group $P4_2/mnm$ are antiferromagnetic insulators, in which the antiferromagnetic superexchange interaction cannot give an outright explanation about the magnetic coupling of Cr atoms.[11–13] Their magnetic structures, namely the Cr–O–Cr magnetic coupling, depend on the X atom. In Cr_2XO_6 (X = W, Mo), the inter-layer Cr atoms are antiferromagnetically coupled, while the neighboring intra-bilayer Cr atoms are ferromagnetically aligned. However, the neighboring intra-bilayer Cr atoms are antiferromagnetically aligned in Cr_2TeO_6. The novel intra-bilayer ferromagnetic coupling can be explained by assuming a virtual transfer between O and W (Mo) atoms which tunes the orbital hybridization between Cr-d and O-p orbitals.[12,13]

Here, we investigate magnetic ordering change of inter-bilayer and intra-bilayer Cr atoms of Cr_2MoO_6 under hydrostatic pressure. The electronic structures are calculated by using Tran and Blaha's modified Becke and Johnson (mBJ) exchange potential, which describes properly the gaps and positions of d electrons of Cr_2MoO_6. The calculated results show that the inter-bilayer magnetic coupling changes from antiferromagnetic coupling to ferromagnetic, and the intra-bilayer coupling changes from ferromagnetic ordering to antiferromagnetic. When the magnetic phase transition happens, a semiconductor–metal phase transition also occurs. The magnetic phase transition can be understood by the intra-bilayer ferromagnetic coupling mechanism proposed by Zhu *et al*. in Refs. [12] and [13].

The rest of the paper is organized as follows. In the next section, we shall give our computational details. In Section 3, we shall present our main calculated results and analysis. Finally, we shall give our conclusion in Section 4.

2. Computational detail

We use the full-potential linearized augmented-plane-waves method within the density functional theory (DFT)[14,15] as implemented in the package WIEN2k.[16] We use the mBJ exchange potential plus local density approximation (LDA) correlation potential for the exchange–correlation potential[17] to do our main electronic structure calculations, and use the popular generalized gradient approximation of Perdew, Burke, and Ernzerhof (GGA-PBE)[18] to optimize the internal position parameters with a force standard of 2 mRy/a.u. The full relativistic effects are calculated with the Dirac equations for the core states, and the scalar relativistic

*Project supported by the Fundamental Research Funds for the Central Universities, China (Grant No. 2015XKMS073).

†Corresponding author. E-mail: guosd@cumt.edu.cn

© 2016 Chinese Physical Society and IOP Publishing Ltd

approximation is used for the valence states.[19–21] The atomic sphere radii of Cr, Mo, and O are chosen to be 1.82 a.u., 1.78 a.u., and 1.61 a.u., respectively. We use a $11 \times 11 \times 6$ Monkhorst–Pack k-points grid for the self-consistent calculation and make harmonic expansion up to $l_{\max} = 10$ in each of the atomic spheres, and set $R_{\mathrm{mt}}k_{\max} = 7$. The self-consistent calculations are considered to be converged when the integration of the absolute charge-density difference between the input and the output electron densities is less than $0.0001|e|$ per formula unit, where e is the electron charge.

3. Results and analysis

The Cr_2MoO_6 has an inverse-trirutile structure with the lattice parameters $a = b = 4.58717$ Å and $c = 8.81138$ Å at $T = 4$ K, which undergoes a paramagnetic–antiferromagnetic transition at $T = 93$ K with inter-bilayer antiferromagnetic coupling and intra-bilayer ferromagnetic coupling.[13] The sketch map of Cr_2MoO_6 crystal structure is shown in Fig. 1. The experimental crystal structure is used as a reference. The hydrostatic pressure is simulated by using V/V_{exp}, where V_{exp} is the volume of the experimental crystal structure. The calculations are performed at six different V/V_{exp}, and the six calculated points are labeled as A (1.0), B (0.97), C (0.94), D (0.91), E (0.88), and F (0.85). Four different magnetic configurations denoted as A–B (AF–AF, F–AF, AF–F, and F–F) are considered, where A represents the inter-bilayer magnetic ordering and B represents the intra-bilayer magnetic ordering. In all calculations, the ionic positions are relaxed by using GGA-PBE. The magnetic energy differences as a function of V/V_{exp} are plotted in Fig. 2. The results show that the AF–F magnetic configuration with the experimental crystal structure is the ground state, which agrees well with the experiment and other GGA or GGA + U calculations.[13] As the volume decreases, the magnetic energy difference between F–AF and AF–F magnetic configurations becomes negative, which implies a magnetic phase transition. The V/V_{exp} corresponding to the magnetic phase transition is about 0.882, and the ground state at A, B, C, and D points has the AF–F magnetic configuration, while the ground state at E and F points has the F–AF magnetic configuration. The magnetic energy differences also show that the F–F magnetic configuration is most unstable under the considered pressure.

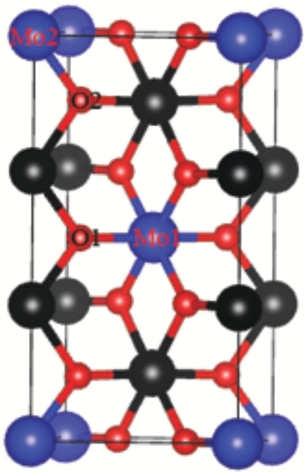


Fig. 1. (color online) The sketch map of Cr_2MoO_6 crystal structure. The black balls, blue balls, and red balls represent Cr atoms, Mo atoms, and O atoms, respectively. The Cr bilayers are separated by a Mo layer. The O atoms connecting inter-bilayer Cr atoms are marked as O1, and the O atoms connecting intra-bilayer Cr atoms are marked as O2. The labeled Mo1 and Mo2 atoms are equivalent.

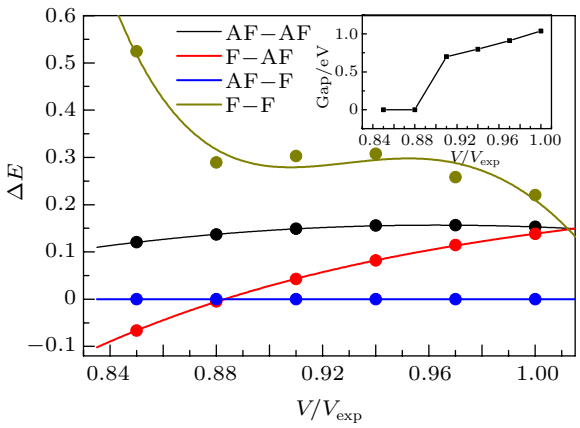


Fig. 2. (color online) The magnetic energy differences as a function of V/V_{exp} (AF–F magnetic configuration is used as a reference). The points represent calculated values, and the lines are obtained by linear or curve fitting. The inset shows the energy band gap as a function of V/V_{exp}.

As is well known, GGA generally does not accurately describe the position of transition-metal d electrons, and underestimates the gaps of magnetic insulators. The improved mBJ exchange potential has been proved to be very effective to describe electronic structures and gaps of magnetic insulators.[5,22–25] The projected spin-dependent densities of states of Cr_2MoO_6 calculated by using mBJ and GGA are shown in Fig. 3. An obvious gap near the Fermi level is produced by using mBJ with respect to the GGA results, and another gap between Mo-d and Cr-d states in the conduction bands is opened. The calculated energy band gap is about 1.04 eV by using mBJ. It is clearly seen that the widths of the d character bands with mBJ become narrower than the ones with GGA. These results are in accordance with the related experiment and the GGA + U calculations in Ref. [13]. The calculated Cr magnetic moment is 2.26 μ_{B} by using GGA, and 2.50 μ_{B} with mBJ (the magnetic moment depends on the chosen atomic sphere radius of Cr). The mBJ result is closer to the experiment value 2.47 μ_{B} with respect to the GGA one. So, we use mBJ to study the electronic structures of Cr_2MoO_6 under hydrostatic pressure. The ground-state total densities of states of Cr_2MoO_6 are plotted in Fig. 4. Figures 4(a)–4(d) correspond to points A–D with AF–F magnetic ordering, and figures 4(e) and 4(f) correspond to points E and F with F–AF

magnetic ordering. Because of the long-range ordered antiferromagnetic state of Cr_2MoO_6, the majority and minority channels are symmetric, and only the majority channel is shown. As the pressure increases, the energy band gap gradually decreases. When V/V_{exp} equals 0.88, the energy band gap disappears, which means a semiconductor–metal phase transition.

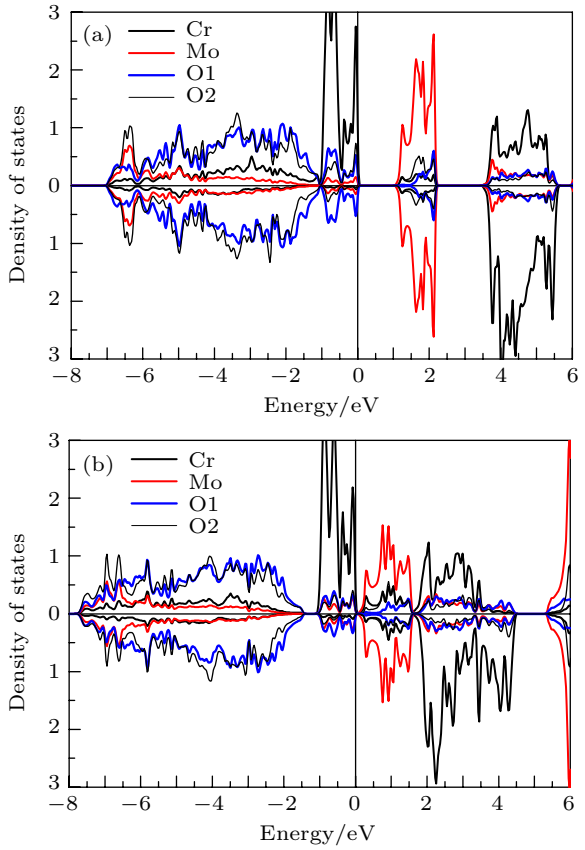


Fig. 3. (color online) The partial spin-dependent densities of states of Cr_2MoO_6 projected in Cr, Mo, O1, and O2 atom spheres by using (a) mBJ and (b) GGA, respectively.

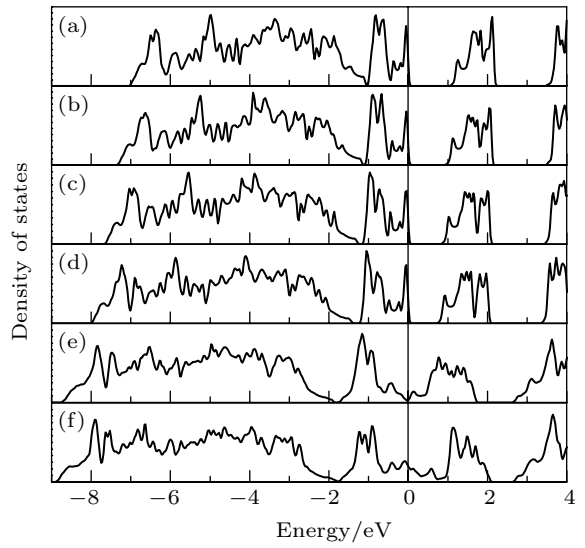


Fig. 4. The total densities of states of Cr_2MoO_6 with (a)–(d) AF–F and (e)–(f) F–AF magnetic configurations by using mBJ. Panels (a)–(f) correspond to points *A*–*F*, respectively.

The energy band gap as a function of V/V_{exp} is plotted in Fig. 2. With the increasing pressure, the gap shows a linear decrease with AF–F magnetic ordering. When the AF–F magnetic ordering changes into the F–AF one, the gap disappears, leading to a semiconductor–metal phase transition.

In Refs. [12] and [13], the mechanism of the intra-bilayer ferromagnetic coupling was explained as follows. The virtual hopping of an O2-p electron to the empty Mo2-d states makes the O2-p state partially occupied, which creates a virtual hole in the O-p band and leads to ferromagnetic coupling between intra-bilayer Cr atoms. The hybridization strength between O1 (O2) and Mo1 (Mo2) is a key factor that determines the inter-bilayer (intra-bilayer) magnetic coupling. Since the distance between O1 and Mo1 and that between O2 and Mo2 control the hybridization strength, we plot the bond lengths of O1–Mo1 and O2–Mo2 (and their average values) as a function of V/V_{exp} with AF–F and F–AF magnetic configurations in Fig. 5. With the increasing of pressure, d_1 decreases more quickly than d_2 with both AF–F and F–AF magnetic configurations. To consider the combined effect of the two kinds of magnetic configurations, the average value of d_1 and d_2 is used to decide the hybridization strength of O and Mo. In Fig. 5(c), it is clearly seen that d_1 becomes smaller than d_2 with the pressure increasing, and then magnetic phase transition occurs. So, the hybridization strength between O and

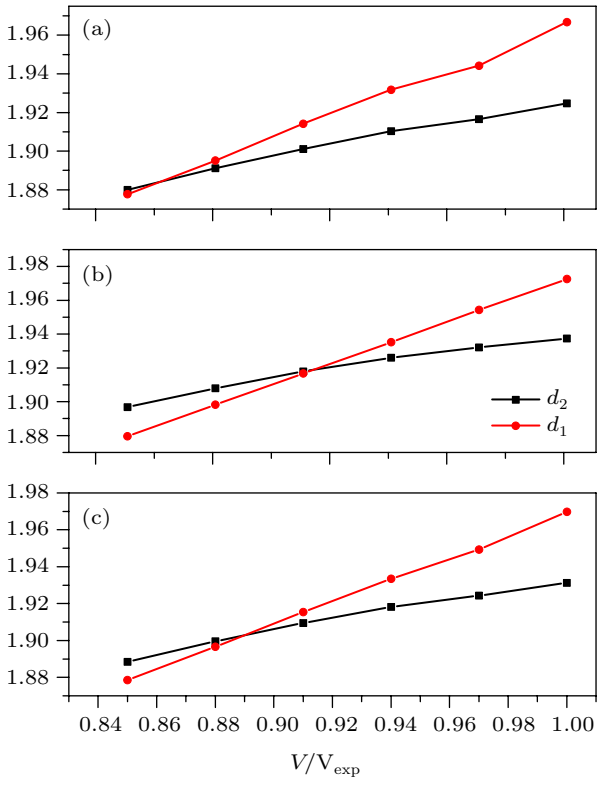


Fig. 5. (color online) The bond lengths of O1–Mo1 (d_1) and O2–Mo2 (d_2) as a function of V/V_{exp} with (a) AF–F and (b) F–AF magnetic configurations, and (c) their average values.

Mo controls the magnetic configuration of Cr_2MoO_6, and if the hybridization strength between O2 (O1) and Mo2 (MO1) is stronger than the one between O1 (O2) and Mo1 (Mo2), Cr_2MoO_6 will possess the AF–F (F–AF) magnetic configuration.

To see clearly the magnetic ordering, we show the magnetization density distributions of Cr_2MoO_6 at points *A* (AF–F) and *F* (F–AF) with energy ranging from −8 eV to the Fermi level in Fig. 6, within the magnetization density −0.01–0.01 μ_B/Bohr^3. Here, the plane is defined by a Cr1–Cr2–Cr3 triangle. The magnetization densities of the nearest O1 related with Cr1 and Cr4 (inter-bilayer coupling) with AF–F are very similar to the ones of the nearest O2 related with Cr1 and Cr2 (intra-bilayer coupling) with F–AF, and the related Cr couplings are all antiferromagnetic. It is clearly seen that the hybridizations among Cr1, Cr4, O1, and Mo1 at point *F* (F–AF) are very obvious, and the Cr and Mo1 spin densities are the same and opposite to the O1 spin densities, which agrees well with the mechanism of the ferromagnetic coupling in Refs. [12] and [13].

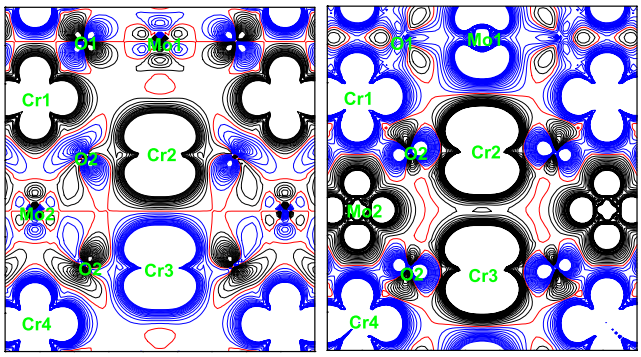


Fig. 6. (color online) The magnetization density distributions of Cr_2MoO_6 at (a) *A* (AF–F) and (b) *F* (F–AF) points. The plane is defined by a Cr1–Cr2–Cr3 triangle. The actual magnetization density is −0.01–0.01 $|e|$/Bohr^3 and the density increment is 0.00067 $|e|$/Bohr^3. The blue, black, and red lines stand for positive, negative, and zero values, respectively.

4. Conclusion

The improved mBJ exchange potential is used to investigate the electronic structures of Cr_2MoO_6 under pressure. The x-ray emission spectra of delafossite type oxide $CuFeO_2$ (magnetic insulator) calculated by using mBJ are quite compatible with the experimental data.[22] The mBJ gives an appropriate description for $HgCr_2Se_4$, $CdCr_2S_4$, and $CdCr_2Se_4$ (magnetic insulator), and the mBJ gaps agree well with the experimental values.[5] So, the mBJ may be suitable to study the electronic structures of Cr_2MoO_6 under pressure.

We investigate the change of magnetic ordering and gaps of Cr_2MoO_6 under pressure. The calculated results show that magnetic and semiconductor–metal phase transitions in Cr_2MoO_6 are caused by the pressure. With the increasing pressure, the AF–F magnetic configuration transforms into the F–AF one, followed by a semiconductor–metal phase transition. The proposed mechanism of intra-bilayer ferromagnetic coupling in Cr_2MoO_6[12,13] can be used to understand the magnetic phase transition, and the Mo–O hybridization strength plays a key role in determining the inter-bilayer and intra-bilayer magnetic ordering. We use the trend of bond lengths of Mo1–O1 and Mo2–O2 under pressure to explain the magnetic phase transition. The idea that empty Mo-d states by perturbing the O-p states can give rise to ferromagnetic coupling between two Cr atoms is further confirmed.

Acknowledgements

We are grateful to the Advanced Analysis and Computation Center of CUMT for the award of CPU hours to accomplish this work.

References

[1] Nayak A P, Bhattacharyya S, Zhu J, Liu J, Wu X, Pandey T, Jin C Q, Singh A K, Akinwande D and Lin J F 2014 *Nat. Commun.* **5** 3731
[2] Li W, Wei X Y, Zhu J X, Ting C S and Chen Y 2014 *Phys. Rev. B* **89** 035101
[3] Xi X X, He X G, Guan F, Liu Z X, Zhong R D, Schneeloch J A, Liu T S, Gu G D, Xu D, Chen Z, Hong X G, Ku W and Carr G L 2014 *Phys. Rev. Lett.* **113** 096401
[4] Xi X X, Ma C L, Liu Z X, Chen Z Q, Ku W, Berger H, Martin C, Tanner D B and Carr G L 2013 *Phys. Rev. Lett.* **111** 155701
[5] Guo S D and Liu B G 2012 *J. Phys.: Condens. Matter* **24** 045502
[6] Anderson P W 1950 *Phys. Rev.* **79** 350
[7] Zener C 1951 *Phys. Rev.* **82** 403
[8] Akamatsu H, Kumagai Y, Oba F, Fujita K, Murakami H, Tanaka K and Tanaka I 2011 *Phys. Rev. B* **83** 214421
[9] Toyoda M, Yamauchi K and Oguchi T 2013 *Phys. Rev. B* **87** 224430
[10] Fennie C J and Rabe K M 2006 *Phys. Rev. Lett.* **97** 267602
[11] Kunnmann W, Placa S L, Corliss L M, Hastings J M and Banks E 1968 *J. Phys. Chem. Solids* **29** 1359
[12] Zhu M, Do D, Dela Cruz C R, Dun Z, Zhou H D, Mahanti S D and Ke X 2014 *Phys. Rev. Lett.* **113** 076406
[13] Zhu M, Do D, Dela Cruz C R, Dun Z, Cheng J G, Goto H, Uwatoko Y, Zou T, Zhou H D, Mahanti S D and Ke X 2015 *Phys. Rev. B* **92** 094419
[14] Hohenberg P and Kohn W 1964 *Phys. Rev.* **136** B864
[15] Kohn W and Sham L J 1965 *Phys. Rev.* **140** A1133
[16] Blaha P, Schwarz K, Madsen G K H, Kvasnicka D and Luitz J 2001 *WIEN2k, an Augmented Plane Wave + Local Orbitals Program for Calculating Crystal Properties* (Karlheinz Schwarz Technische Universityät Wien, Austria)
[17] Tran F and Blaha P 2009 *Phys. Rev. Lett.* **102** 226401
[18] Perdew J P, Burke K and Ernzerhof M 1996 *Phys. Rev. Lett.* **77** 3865
[19] MacDonald A H, Pickett W E and Koelling D D 1980 *J. Phys. C* **13** 2675
[20] Singh D J and Nordstrom L 2006 *Plane Waves, Pseudopotentials and the LAPW Method* (2nd Edn.) (New York: Springer)
[21] Kunes J, Novak P, Schmid R, Blaha P and Schwarz K 2001 *Phys. Rev. B* **64** 153102
[22] Guo S D 2015 *J. Magn. Magn. Mater.* **377** 226
[23] Guo S D 2015 *Eur. Phys. J. B* **88** 82
[24] Song Z W and Liu B G 2013 *Chin. Phys. B* **22** 047506
[25] Guo S D 2014 *Chin. Phys. Lett.* **31** 017101